RESEARCH PAPER

Anticancer activity of synthesized Ag-doped CuO nanoparticles using *Ephedra intermedia* plant against PC-3 prostate cancer cell line

Parisa Raisi Dehkordi [1], Azadeh Mohammadgholi [1]*, Nastaran Asghari Moghaddam [1]

[1]Department of Biology, Central Tehran Branch, Islamic Azad University, Tehran, Iran

ABSTRACT

Objective(s): This research was done to synthesize Ag-doped copper (CuO) nanoparticles (NPs) using the *Ephedra intermedia* plant and investigate its anticancer properties against the PC-3 prostate cancer (PC) cell line.
Materials and Methods: Ag-doped-Cu NPs were biologically synthesized using E.intermedia extract. The synthesized Ag-doped-Cu NPs were characterized using X-ray diffraction (XRD), CuK radiation and fourier-transform infrared spectroscopy (FT-IR), dynamic light scattering (DLS), transmission and scanning electron microscopy (TEM and SEM, respectively) as well as energy dispersive X-ray (EDAX). The expression of *Bax*, *Bcl2*, *P53*, and *caspase-3* genes was evaluated by Real-time PCR (RT-PCR) and apoptosis was assayed using Annexin-V kit. Also, the production of reactive oxygen species (ROS) was estimated at 1000 RFU and 1500 RFU in PC-3 cells treated with extract and green-synthesized Ag-doped-Cu NPs.
Results: The particles were in nano size (55.24-84.41 nm) and the XRD test proved the crystalline structure of NPs. EDAX analysis confirmed the presence of Cu, C, and Ag elements. The results of gene expression showed that the IC_{50} concentration of the doped NPs makes a significant increase in the *Bax*, *caspase-3*, and *P53* expression levels and a significant decrease in the *Bcl2* expression compared to the reference gene and the extract-treated cells. Treatment with doped NPs induced more apoptosis and necrosis than that of treatment with extract. Also, a remarkable enhancement in nitric oxide (NO) enzyme levels was found in the doped NPs compared to the extract alone.
Conclusion: This study proves that the doped NPs induce apoptosis by affecting the expression of pro-apoptotic genes and ROS over-production.

Keywords: Anticancer properties, Apoptotic properties, Ag-doped CuO NPs, Ephedra intermedia, PC-3 prostate cancer cell line

INTRODUCTION

Cancer is one of the most common and fatal diseases in the world. A member of the top five leading causes of death due to cancer globally is prostate cancer (PC) [1, 2]. A total of 174,650 new PC cases was identified in 2019, making up 20% of all new cancer diagnoses in males [3]. PC patients frequently receive chemotherapy, which works to get rid of cancer cells that divide quickly. Nanoparticles (NPs) show potential as

a viable therapeutic strategy for PC because of their capacity to effectively target solid tumors by leveraging tumor permeability as well as retention [4]. Given their extremely small size, NPs avoid non-targeted treatment-related negative effects following systemic delivery while also boosting the effectiveness of the packed anticancer drugs. Additionally, NPs are capable of actively targeting tissues when combined with receptor-targeting compounds [5, 6]. Biogenic silver NPs (AgNPs) have anti-oxidant, antibacterial, antifungal, and DNA- cleaving properties [7]. AgNPs have significant effects on medical diagnosis, treatments, antioxidant, antibacterial, and cytotoxic characteristics, among many others. The

ability of copper oxide nanoparticles (CuO NPs) to destroy cancer cells has captured the attention of all researchers because of its extended lifespan and high cost-effectiveness. CuO NPs exhibit unique chemical, thermal, and biological characteristics [8]. Reactive oxygen species (ROS), which may be produced by mitochondria and phagocytes as well as on the surface of NPs, are currently thought to be the main cause of AgNPs toxicity. Apoptosis is a strictly controlled physiological process that clears the body of extraneous, aberrant, deteriorating, or damaged cells. In addition to the generation of ROS and mitochondrial dysfunction triggered by AgNPs, it has also been shown that cells lose glutathione, an antioxidant, superoxide dismutase, and lactate dehydrogenase, released into the extracellular space when cell membranes are damaged [9]. Ag and Cu NPs exhibit remarkable anticancer activity. They induce cytotoxicity by disrupting cancer cell membranes, interfering with cellular processes, and promoting apoptosis. The exact mechanism involves several factors: (1) ROS: metal NPs generate ROS leading to induce oxidative stress and DNA damage in cancer cells, (2) DNA interaction: Ag and Cu NPs can bind to DNA, and affect gene expression and cell survival, (3) Mitochondrial dysfunction: NPs disrupt mitochondrial function, impair energy production, and promote cell death, (4) Cell membrane interaction: NPs interact with cell membranes and cause membrane damage and cell lysis, (5) Apoptosis induction: Ag and Cu NPs trigger apoptotic pathways, leading to programmed cell death [10-12].

Other scientists have developed NPs from natural sources including plants, fungi, yeast, and bacteria. Plants are abundant in phytochemicals with bioactive properties that can inhibit and stop the growth of cancer [13]. In actuality, a number of the most popular chemotherapy treatments originate in plants. The traditional physical and chemical procedures for making NPs employ poisonous and dangerous substances. The green biosynthesis of NPs, on the other hand, provides a quick, practical, scalable, and environmentally friendly substitute that uses less energy [14]. The goal of the current work was to use *E. intermedia* leaf extract to synthesize silver-doped copper oxide nanoparticles (Ag-doped CuO NPs) as an environmentally acceptable approach. The plant extract is an important source of polyphenolic components, which gives it substantial antioxidant effects, in addition to this family of phytochemicals.

Additionally, one of the main parts of this plant is essential oil. Ephedra species have been shown to exhibit antioxidant, antibacterial, antifungal, and anticancer activities [15, 16]. To examine the antioxidant properties, pro-apoptotic, anti-proliferative, and cytotoxic effects against the PC-3 PC cell line, we have synthesized Ag-doped CuO NPs using *E. intermedia* plant, which is rich in flavonoids and polyflavonoids. The aqueous extract of *E. intermedia* has been revealed the existence of several phytochemicals that are significant for therapeutic purposes [17]. Synthesized *E. intermedia*-AgNPs has been showed significant antibacterial ability against a range of pathogenic bacterial and fungus strains. Furthermore, *E. intermedia*-AgNPs has been showed evidence of cytotoxic action on human liver cancer cells [18]. The biological potential of *E. intermedia* indicates that it may be useful in treating degenerative, cancer, and microbial diseases. By inducing apoptosis, the tested samples treated against human lung cancer A549 cells demonstrated inhibition in cell proliferation and enhanced morphological and cytological alterations via an increased level of ROS accumulation in the NSCLC cell line. These findings were obtained through the use of Ag-doped CuO NPs [19]. Drug-resistant PC cells (DU145-TXR) have been exposed to $Cu(DDC)_2$ NPs, which caused paraptosis, a nonapoptotic form of cell death [20]. Ag-doped CuO NPs with *Moringa oleifera* leaf extract has been used to treat human lung cancer cells A549 and inhibited cell proliferation and improved morphological and cytological changes due to increased ROS accumulation in NSCLC cell line [19]. Prashanth et al. have compared the anticancer effect of Ag/CuO NCs and CuO NPs on cancer cell line MDA-MB-231. The anti-mycobacterial activity of the NPs against four mycobacterium species has proved that Ag/CuO NCs have higher anticancer than the undoped CuO NPs [21]. Besides, a hybrid of silver-copper oxide nanocomposites (Ag–CuO NCs) has been applied to affect the growth of *Tetraselmis suecica*, a marine microalgae species; and the results clarified the variations in the amount of chlorophyll and growth reduction, dependent on both time and dose. These materials were particularly successful in reducing the growth of the A549 lung cancer cell line [22]. Due to the demand needed for more investigation, we have synthesized Ag-doped CuO NPs using *E. intermedia* [23]. Based on the survey that has been done on NPs and *E.*

intermedia extract, the effect of Ag-doped CuO NPs on the PC-3 cell line was investigated. MTT assay, Real-Time PCR (RT-PCR), flow cytometry, ROS level, and NO production were carefully analyzed in three cell lines including control group, treated one only by the extracts, and treated one by NPs from *E. intermedia*. The primary objective of our study is to investigate the anticancer activity of synthesized Ag-doped CuO NPs using the *E. intermedia* plant extract. By employing a green synthesis method, we have aligned with current trends in nanotechnology and contributed to sustainable approaches. Specifically, we aimed to evaluate the cytotoxic effects of these NPs against the PC-3 PC cell line. Our work addresses the need for effective and targeted cancer therapies, emphasizing the unique properties of Ag-doped CuO NPs. Our research stands out due to several novel aspects. First, we have employed green synthesis by utilizing plant-derived compounds for NP production, minimizing environmental impact, and promoting eco-friendliness. Second, the incorporation of Ag into CuO NPs enhances their properties, potentially improving their efficacy as therapeutic agents. Lastly, our focus on the PC-3 PC cell line allows us to explore selective cytotoxicity, addressing a specific clinical need and contributing to the advancement of cancer treatment strategies.

MATERIAL AND METHODS

Synthesizing Ag-doped CuO NPs using E. intermedia

The *E. intermedia* plant was achieved from the plant bank of the Iranian Center for Biological Resources, and then approved by the Department of Botany under the IBRC barium number P1006547. To prepare the extract, the aerial sections of the *E. intermedia* were firstly placed in the air and then completely dried in the shade. The leaves were completely powdered by an electric grinder and stored in glass containers. The prepared powder was used for extraction by the Soxhlet method. In this way, 50 g of plant leaf powder was mixed with 500 mL of aqueous solvent. Extraction was done for 12 hr and at the end, the solvent was isolated using a rotary evaporator (Rv10 digital, Germany). The achieved solid powder was brought to volume by double distilled water (DW) and the obtained extract was stored at 4°C until use to investigate the effect on cancer cells [24]. To prepare Ag-doped-Cu NPs, the

amount of 0.01 M copper sulfate ($CuSO_4$) (Merck, Germany) was mixed with 0.1 M of silver nitrate (AgNO3) (Merck, Germany) in 100 mL of DW and mixed with 4-5 mL of extract. The mixture was stirred for overnight. Synthesis of AgNPs doped with Cu was confirmed by color change. The sediment was washed three times using DW. In all washing stages, the solutions were centrifuged at 13000 rpm for 20 min. Finally, the final washing was done with ethanol and the product was placed at 60°C for 2 hr. The product was placed at 37 °C for 4 hr.

Characterization of Ag-doped CuO NPs

The hydrodynamic particle size distribution of Ag-doped CuO NPs was evaluated by DLS (Malvern Zeta Sizer, Malvern Instrument Ltd. Malvern, UK). The crystal phase of Ag-doped CuO NPs powder was examined by XRD (PW3710, the Netherlands) using CuK radiation (= 0.0260 nm). The presence of major functional groups of phytochemicals as well as molecular binding properties of *E. intermedia* and Ag-doped CuO NPs was approved by FT-IR analysis (Spectrum Two, USA). TEM (EM10C-100 KV Zeiss, Germany), SEM (FEI NOVA NANOSEM 450, at an accelerating voltage of 15 kV), and EDX Analyzer (EDX, JSM-7500 Field Emission Scanning Electron Microscope (Japan) coupled to an EDAX analyzer) were applied to determine the particle size, shape, and elemental composition of biogenic of Ag-doped CuO NPs. The absorption spectra of the synthesized samples (Ag-doped CuO NPs) were obtained using a Shimadzu-UV 1800 UV-Vis spectrometer.

PC-3 cell culture and cytotoxicity test

The PC-3 human PC cell line was prepared by the Iranian Biological Resource Center. The PC-3 cells were grown at 37 °C and 5% CO_2. The cells were cultured in fresh media (RPMI1640) treated with 10% fetal bovine serum (FBS, Gibco, USA) and 1% antibiotics (streptomycin/penicillin, Gibco, Waltham, MA, USA), all cell line was tested for mycoplasma contamination. When PC-3 cells were subjected to the different concentrations of the Ag-doped CuO NPs, the 3-(4,5-dimethylthiazol-2-yl)-2,5-diphenyltetrazolium bromide (MTT) assay was used to measure cell growth activity and cytotoxicity. Twenty four hours after incubation, cell viability was evaluated by the MTT test using 96-well plates, which was carried out by protocol. In brief, $1×10^4$ PC-3 cells were seeded

onto the plates, followed by incubation at 37°C in a humidified 5% CO_2 environment until 60% confluency. Before treatment, the cells were undergone 24 hr of serum fasting and after the whole growth, media was withdrawn. The cells were incubated in culture media for 2 hr on their own as the control (untreated cells). The *E. intermedia* extract and the Ag-doped CuO NPs were added to the cells (treated groups) at the different levels (3.125, 6.25, 12.5, 25, 50, and 100 μg/mL). The medium was then taken out, and 100 μL of MTT solution was applied to all wells followed by incubation for 4 h at 37 °C with 5% CO_2. After removing the MTT solution, 200 μL aliquots of dimethyl sulfoxide (DMSO, Merck Chemical Co. (Darmstadt, Germany) were poured into the wells to disintegrate the formazan crystals and the wells were then incubated at 37 °C for 10 min. The treatments were carried out three times, and optical densities (OD) were assessed spectrophotometrically (ELISA Reader [Organon Teknika, Oss, Netherlands]) at 570 nm. A statistical program (Pharm-PCS software) was used to determine the IC_{50} of extract and biosynthesized NPs on PC-3 cell lines [25].

Evaluation of Bax, Bcl2, P53, and caspase-3 expression by RT-PCR

RNA was extracted from the cells by an RNX kit (available from Cinnagen Co. in Iran). To determine the amount and purity of RNA, a spectrophotometer was used to detect an RNA sample absorbance at 260 and 280 nm. RNase-free DNase I (from Thermo Scientific) was used to extract genomic DNA. As instructed, 2 μg of the treated RNA with IC_{50} concentration of anticancer agents was used in a RT-PCR technique to perform the cDNA synthesis reaction using Fermentas First Strand cDNA Synthesis Kit. The gene expression was then evaluated using 1 μg of cDNA and certain primers (Table 1). The amplification was done on the ExicyclerTM 96—Bioneer (South Korea) in a reaction volume of 25 μL using 0.5 μM of each primer, 12.5 μL of the SYBR Green kit (Amplicon, Denmark), and 1 μg of cDNA. The temperature schedule was fixed at 95 °C for 1 min, 95 °C for 15 s, and 60°C for 1 min. As an internal control, the *β--actin* gene was used. The $2^{-\Delta\Delta CT}$ approach was used in the present research to assess the relative alterations in expression levels resulting from quantitative RT-PCR tests.

Table 1. Designated primer sequence for the RT-PCR process.

Gene	Primer sequence
b-actin	Forward: 5'- TCCTCCTGAGCGCAAGTAC-3'
	Revers: 5'- CCTGCTTGCTGATCCACATCT-3'
Bax	Forward: 5'- GAGCTGCAGAGGATGATTGC-3'
	Revers: 5'- AAGTTGCCGTCAGAAAACATG-3'
Bcl2	Forward: 5'- ATTGGGAAGTTTCAAATCAGC-3'
	Revers: 5'- CAGTCTACTTCCTCTGTGATGTTG-3'
P53	Forward: 5'- TAACAGTTCCTGCATGGGCGGC -3'
	Revers: 5'- AGGACAGGCACAAACACGCACC -3'
Casp3	Forward:5'-CATACTCCACAGCACCTGGTTA-3'
	Revers: 5'-ACTCAAATTCTGTTGCCACCTT-3'

Apoptosis assay of the Ag-doped CuO NPs

The susceptibility of PC-3 cells to apoptosis was assessed using Annexin-V-FITC/propidium iodide labeling (annexin V-FITC flow cytometry kit was obtained from Affymetrix Biosciences, ThermoFisher Scientific). The cells were treated with IC_{50} concentration of plant extract and the Ag-doped CuO NPs for 24 hr by the directions provided by the manufacturer. Then, the cells were collected and washed twice using PBS. We set the cell suspension to 5×10^5 cells/mL (seeded in a 6-well plate) in 1x binding buffer. The Apoptosis Quantitation Kit was used to get rid of the cells with two different substances, Annexin V - FITC and Propidium - Ithaca. Annexin-V-FITC (5 μL) attaches to the surface of the apoptotic cell and emits green light. Propidium Ithaca breaks down the membranes of the necrotic cell and interlinks with DNA, giving off red light. The percentage of each type of cell (apoptotic and necrotic) was determined using a functional flow cytometer.

ROS (H2-DCFH-DA) assay

The amount of oxidative stress (ROS) produced by the samples was measured using the 2', and 7' -DHCDFDA kit (ROS Assay Kit, Abcam Company, Cambridge, United Kingdom]). The 2'-DHCDFDA acetyl esters, which were created by reducing the DCFDA, exhibited fluorescence at 530 nm. This fluorescence could be indicative of oxidative stress. The PC-3 PC cells were treated with IC_{50} samples for 24, washed with PBS and then incubated at 37 °C for 30 min with 80 mM of 2'-DHCDFDA.

A microplate reader was sued to measure the fluorescence (ELISA Reader, Organon Teknika, Oss, Netherlands) [26].

Nitric oxide activity level

A Natrix kit (Arman Biotech Co, Iran) was used to measure the NO enzyme in cancer cells treated with IC_{50} concentration of the *E. intermedia* extract and the Ag-doped CuO NPs. In general, after removing the culture medium by centrifugation, 2×10^6 cells were homogenized in 200 µL of PBS (pH=7.4), followed by centrifugation for 10 min at 13,000 rpm. For protein precipitation, 150 µL of the sample with 80 µL of buffer A (Buffer A) was vortexed and 80 µL of buffer B then added. Following mixing, it was centrifuged at 14,000 rpm for 10 min and the supernatant was separated. Three columns (24 wells) of a 96-well microplate were determined for the nitric standard reference curve. A total of 50 µL of double DW was added to row B-H wells. A total of 100 µL of the prepared standard solution was added to the remaining 3 wells in row A, and then, 50 µL from the upper well (row A) was added to the lower well. This work was continued serially until row G for the concentrations 100, 50, 25, 12.5, 6.25, 3.125, and 1.56 µM. To measure NO in the samples, 50 µL of each sample was poured into light-colored wells and 50 µL of reagent R1 was added to all wells and mixed. Then, it was incubated for 10 min away from light and at room temperature. Following

incubation, 50 µL of R2 reagent was added to all wells and mixed. Ten minutes following mixing the reagents, the plate was read at 570 nm toward the blank well (50 µL R1 + 50 µL R2 + 50 µL DW). Using the obtained results, a standard curve was drawn and applied to measure the NO concentration in the target sample.

Statistical analysis

Data analysis was done by SPSS software (V. 20). The data were analyzed by One-way Analysis of Variance (ANOVA) followed by Tukey's post-hoc-test to assess significant variation among the treatments ($P<0.05$).

RESULTS
Characterization of Ag-doped CuO NPs

The Ag-doped CuO NPs were generated using a plant extract from *E. intermedia* under facile procedures. The average size and PDI obtained by DLS were about 65 nm and 0.204 nm, respectively, for the Ag-doped CuO NPs (Fig. 1) [27]. The particle size dispersion was greater in DLS than in SEM and TEM, which may be due to the formation of the hydrodynamic shell in the aqueous condition for DLS measurement, presumably dependent on NPs composition, roughness, unique shape, and interactions [28].

The morphological and structural characteristics of the Ag-doped CuO NPs were investigated using SEM and TEM. Approximately
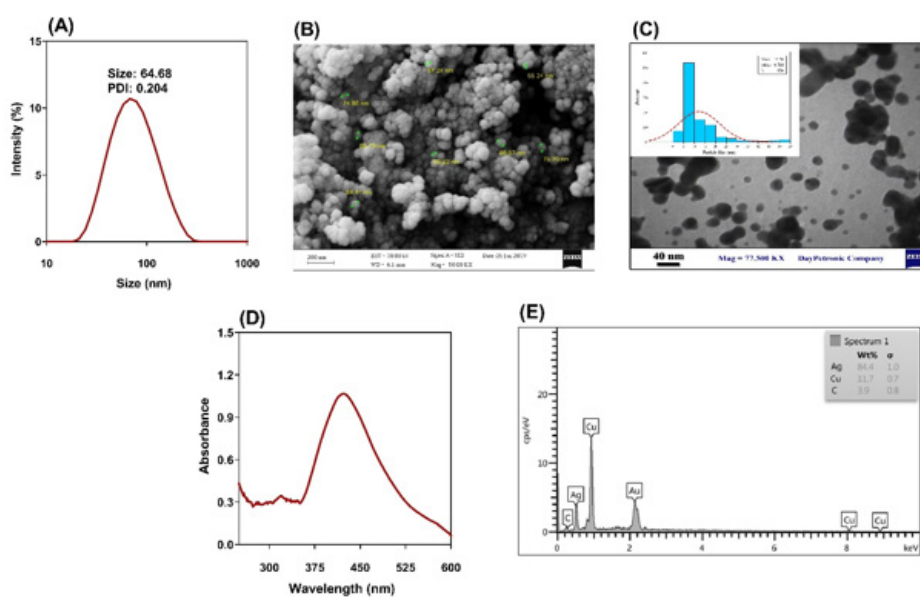

Fig.1. (A) DLS, (B) SEM, and (C) TEM graph of Ag-doped CuO NPs. (D) UV-Vis spectrum, and (E) EDAX tests of doped Ag-doped CuO NPs [27]

a spherical form in the region of 55.24–84.41 nm was observed in the SEM image (Fig. 1B). The TEM image (Fig. 1C) demonstrated the broad size distribution of the NPs. The UV-Vis spectra of the green-synthesized Ag-doped CuO NPs, which give the plasmon resonance at 400 nm, are shown in Fig. 1D. The maximum wavelength of AgNPs was in the region of 350–450 nm. To verify that the elements Ag, C, and Cu were present in the synthesized Ag-CuO NPs, an EDX examination was conducted using an extract from *E. intermedia*. Fig. 1E shows that 84.4% of NPs are composed of Ag elements and 11.7% are composed of Cu ones. .The formation and doping of Ag on Cu is proved by examining the X-ray diffraction pattern. According to Fig. 2A, the peaks corresponding to Cu and Ag are at the angles of 13.85°, 16.54°, 18.04°, 22.78°, 27.87°, 30.65°, 32.25°, 33.41°, 34.48°, 35.68°, 36.57°, 37.79°, 39.69°, 41.33°, 42.28°, 43.39°, 44.88°, 46.23°, 47.65°, 48.36°, 50.05°, 52.61°, 53.55°, 54.79°, 56.31°, 57.76°, 59.12°, 60.16°, 61.66°, 63.53°, 64.36°, 65.18°, 66.78°, 70.33°, 72°, 73.86°, and 76.07°. Ag peaks doped on Cu with the standard peaks in corners and sides 27.84 (111), 32.25 (002), 46.26 022), 54.85 (113), 57.52 (222), and 76.80 (024) with reference code 98-006-0414 and the cubic structure was matched, which confirmed Ag in the structure. On the other hand, Cu peaks in angles and planes are 13.88°(200), 16.54° (210), 18.02° (-201), 22.79° (310), 27.96° (400), 30.59° (230), 33.45° (420), 34.48° (330) , 35.61° (-222), 36.35° (510), 37.70° (-322), 39.76° (520), 41.24° (-232), 42.23° (-512), 43.53° (610), 44.97° (530), 46.08° (-432), 47.63° (-612), 48.29° (250), 50° (-532), 5254° (-442), 53.51° (-712), 54.75° (450), 56.16° (522), 57.68° (-352), 59.19° (-802), 60.12° (-452), 61.56° (-204), 63.42° (-404), 64.42° (014), 65.04° (830), 66.64° (910), 70.31°

(-434), 71.86° (-624), 73.69° (- 244), and 75.77° (-724), corresponding to reference code 00-043-1458 and monoclinic structure, confirms Cu. The size of Ag-CuO NPs crystal was calculated according to the Debye Scherer equation $D = k\lambda/\beta\cos\Theta$, where D is the crystal size, β is the width of the peak at half maximum intensity, θ is the Bragg angle of the peak, and λ is the wavelength of X-rays. According to results, Ag-CuO NPs crystallinity percentage and crystallite size are 6.76% and 668 nm, respectively. The chemical interactions between compounds and elements in the structure of extracts and bio-synthesized NPs were investigated, as presented in Fig. 2B [27]. Obviously, the band formed at 1637 cm^{-1} and 3436 cm^{-1} can be attributed to C=O or C=C vibrations and OH stretching in the structure of the extract, respectively. The peaks at 1123.26, 1452.30, 1740.88, and 2942.84 cm^{-1} correspond to C-H plane bending vibration, C=C aromatic bending, C-O-C stretching, and H-Cl stretching in the structure of green-synthesized NPs, respectively. The multiple peaks formed in the region of 400-700 cm^{-1} are attributed to the presence and interactions of Cu elements. The detected peaks more closely resemble the flavonoids and phenols found in Ephedra species.

Cytotoxicity assessment of Ag-doped CuO NPs

Fig. 3 provides an overview of the main findings when MTT PC-3 cells were exposed to *E. intermedia* and Ag-doped CuO NPs at doses ranging from 3.125 µg/mL to 100 µg/mL for 24 hr. According to the findings, the viability of PC-3 cells was decreased concentration-dependently. Besides, there was a significant decrease in the survival of cancer cells at 50 (P<0.05) and 100 (P<0.01) µg/mL extract, as well as a significant decrease in survival after treatment with all concentrations of green-synthesized NPs
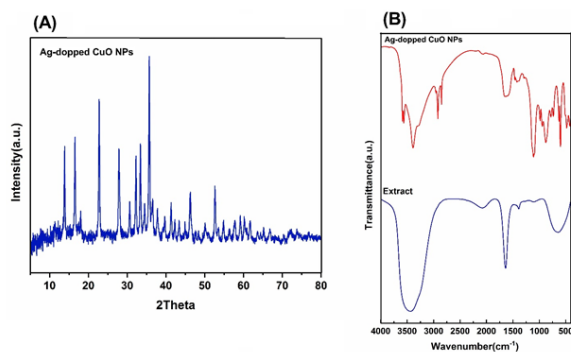

Fig. 2. (A) XRD pattern for Ag-doped CuO NPs. (B) FTIR spectra of Ag-doped CuO NPs and plant extract [27]
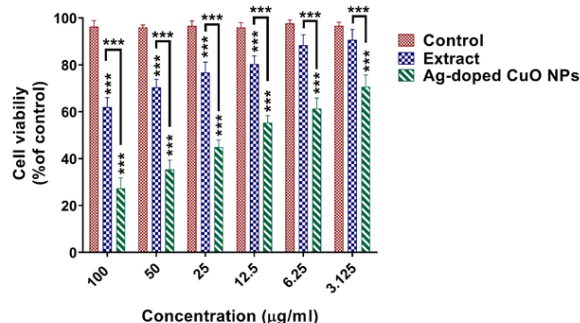

Fig. 3. MTT assay for viability PC-3 cancer cells following treatment with the various concentrations of Ag-doped CuO NPs and *E. intermedia* extract. *:P<0.05, **:P<0.01 and ***:P<0.001
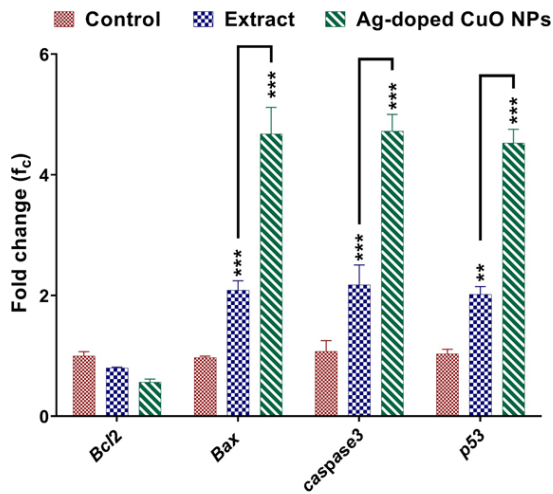
Fig.4. RT-PCR analysis for the expression of *Bax*, *Bcl2*, *Caspase-3*, and *P53* genes in PC-3 cancer cells following treatment with IC_{50} concentration of Ag-doped CuO NPs and *E. intermedia* extract. Data are represented as mean ± SD and n=3; **:$P<0.01$ and ***:$P<0.001$

(P<0.001) compared to the control, which shows that even low concentrations of the synthesized NPs cause a significant decrease in the survival of cancer cells. The highest reduction in cell viability was calculated to be around 28% at 100 µg/mL of the Ag-doped CuO NPs. IC_{50} concentrations for the extract and the synthesized NPs were reported as 374.23 and 17.56 µg/mL, respectively. The portion of alive cells that were treated by the Ag-doped CuO NPs was significantly reduced compared to the cells that were used only extract (P<0.01).

Moreover, the percentage of the alive cells in control group was significantly more than those of two other groups.

Pro-apoptotic and anti-apoptotic gene expression

To improve personalized treatment, researchers study how genes behave in cancer cells. They use a method called reverse transcription-polymerase chain reaction (RT-PCR) to see how cancer cells change after exposure to a test treatment. The Ag-doped CuO NPs could significantly change the *Bax*, *Caspase 3*, *P53*, and *Bcl-2* expression in PC-3 cells compared to the extract and control group (P<0.001) (Fig. 4). In the cells treated to IC_{50} of extract, qRT-PCR findings demonstrated over-expression of *Bax* and *Caspase 3* (two-fold) (P<0.05). The expression of the *P53* and *Bcl2* genes, however, did not alter noticeably between cells exposed to the extract at IC_{50} and the control gene. Additionally, the IC_{50} concentration of the green-synthesized NPs causes a significant increase in the *Bax*, *Caspase-3*, and *P53* expression (approximately 4.5-fold) and a decrease in the *Bcl2* expression compared to the reference gene (P<0.001).

Apoptosis/necrotic ratio in the treated cells

Apoptosis is an indicator of the occurrence of cell death in treated cancer cells, the measurement of which helps to evaluate the anti-cancer effects of treatments. Fig. 5A shows the apoptosis and necrosis in the control cells (untreated), the cells receiving *E. intermedia* extract, and the cells
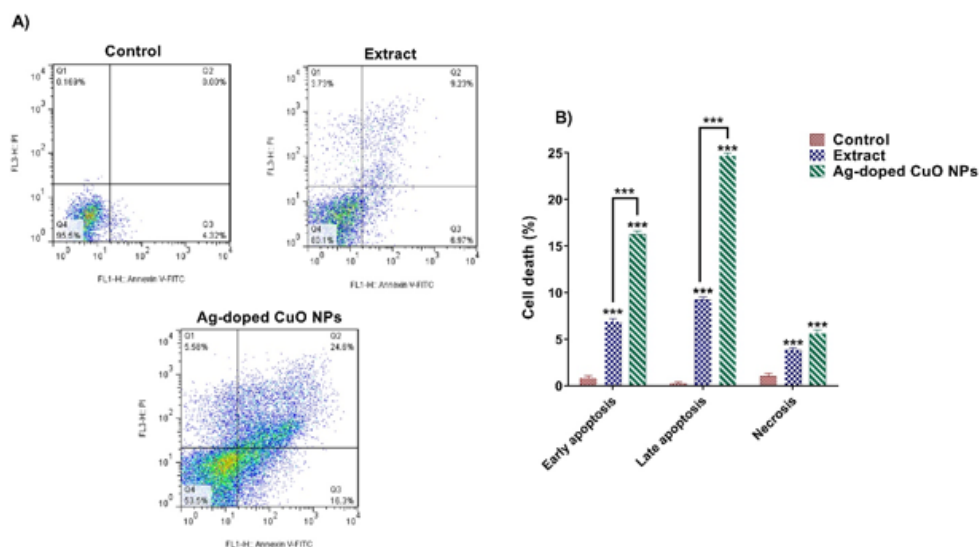

Fig. 5. Flow cytometry analysis for the apoptosis/necrosis ratio in untreated PC-3 cancer cells as control (AI) and in cells treated with IC_{50} concentration of (AII) Ag-doped CuO NPs and (AIII) *E. intermedia* extract. (B) Comparison of early apoptosis, late apoptosis, and necrosis ratio in PC-3 cancer cells following treatment with IC_{50} concentration of Ag-doped CuO NPs and *E. intermedia* extract compared to the untreated group. Data are represented as mean ± SD and n=3; P<0.001***.

treated with the Ag-doped CuO NPs. According to Fig. 5A, 96.4% of the control cells are alive because they were not treated with anticancer agents. After treatment with the extract, 75.5% of the cells enter the early apoptosis phase, 9.09% of the cells enter the late apoptosis phase, and 3.51% of the cells undergo necrosis. Meanwhile, treatment with NPs cause 15.9% early apoptosis, 14.7% delayed apoptosis, and 6.04% necrosis in the cancer cells. Fig. 5B shows that the incidence of early and late apoptosis as well as necrosis was significantly higher in cells receiving both *E. intermedia* extracts and the Ag-doped CuO NPs, while the treatment with green-synthesized NPs cause almost 2 times more apoptosis and necrosis compared to the extract-treated cells (P<0.001).

ROS production

Fig. 6 shows ROS production in the cancer cell lines after treatment with the *E. intermedia* extract and the Ag-doped CuO NPs compared to untreated cells. The production of ROS was estimated at 1000 RFU and 1500 RFU in PC-3 cells treated with extract and the green-synthesized Ag-doped CuO NPs compared to control, respectively, proving the dramatic overproduction of ROS in both treated groups (P<0.001). However, ROS production was significantly higher in the Ag-doped CuO NPs treated cells than that of the extract-treated group (P<0.001).

NO activity in the treated cells

The activity of NO after treatment with extract and the doped NPs was significantly increased compared to the untreated controls (P<0.05 and P<0.001, respectively), and this increase in cells treated with the NPs was almost 4-fold higher than in the cells receiving the extract (P<0.001). (Fig. 7).

DISCUSSION

Metallic NPs that have undergone bio-reduction offer a variety of useful features and are known for being biocompatible. Because of their enhanced responsiveness and effectiveness, caused by their larger surface-to-volume ratio and quantum effects, they have been regarded as significant in the arena of medicine [29]. The synthesis of Ag-doped CuO NPs using plant extracts has shown promising anti-cancer activity in various studies. For instance, green-synthesized CuO NPs have demonstrated potent anti-cancer properties against different cell lines, including MCF-7 and A549 [19, 30]. Additionally, the anti-cancer potential of CuO NPs prepared using plant extracts has been shown to inhibit cancer cell proliferation [31]. Furthermore, hybrid Ag-CuO nanocomposites have outstanding anti-proliferative activity against lung cancer cells, indicating their efficacy in inhibiting cancer progression [23]. Moreover, the green synthesis of stable Ag and CuO NPs induce cytotoxic effects on various cancer cell cultures, including lung, colon, and laryngeal carcinoma cancers, underscoring their potential as anti-cancer
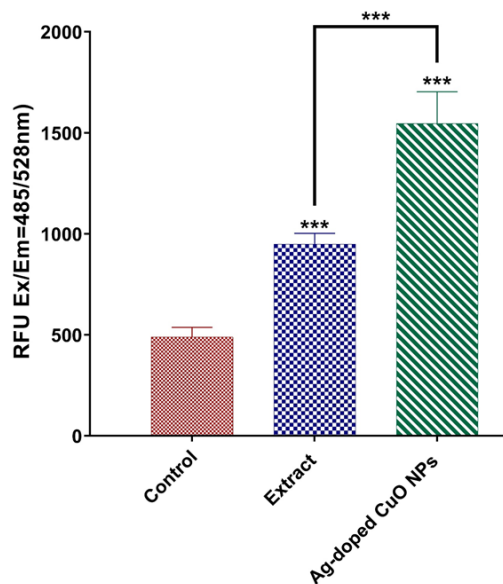

Fig. 6. Comparison of ROS production in PC-3 cancer cells following treatment with IC$_{50}$ concentration of Ag-doped CuO NPs and *E. intermedia* extract compared to the control group. Data are represented as mean ± SD and n=3; P<0.001***
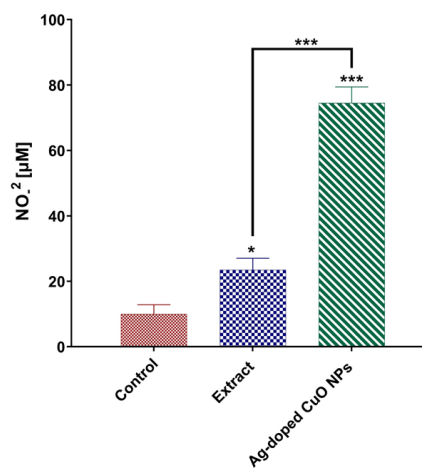

Fig. 7. Comparison of nitric oxide production in PC-3 cancer cells following treatment with IC$_{50}$ concentration of Ag-doped CuO NPs and *E. intermedia* extract compared to the controls. Data are represented as mean ± SD and n=3; *:P<0.05, and ***:P<0.001

agents [32]. Additionally, the green-emitting Cu nanoclusters capped with amino acids are potent as a fluorescence resonance energy transfer pair with anticancer drug doxorubicin, indicating their role as effective drug carriers for targeted drug delivery within the human body [33, 34]. These studies have collectively highlighted the promising anticancer properties of green-synthesized Cu-Ag NPs and Cu nanoclusters, paving the way for further research in utilizing these nanomaterials for cancer treatment. Therefore, utilizing the Ag-doped CuO NPs synthesized from *E. intermedia* plant extracts may hold promise in combating PC-3 cells.

Here, we have evaluated the effectiveness and environmental friendliness of the Ag-doped CuO NPs produced by *E. intermedia* against human PC-3 cells. The presence of several extract metabolites on the surface of doped NPs was verified using characterization methods, XRD, UV-Vis, EDX, and FT-IR analyses. In actuality, the various bioactive chemical components of the *E. intermedia* extract, including aromatic compounds, amides, flavonoids, and amines, acted as bio-reducing agents for the reduction of Ag+ to AgNPs and Cu+ to CuNPs. Additionally, these bioactive substances served as stabilizing/capping agents and catalysts for the redox processes [35]. Through synergistic effects, the presence of these phytochemicals on the NP surface may improve the efficacy of Ag-doped CuO NPs as anti-proliferative treatments. The size, shape, and spacing of the particles we create, as well as the properties of the surrounding material, all affect how surface plasmon absorption occurs [36, 37]. We hypothesized that these secondary metabolites are responsible for both producing and stabilizing Ag-doped CuO nanoparticles [38].

The lethal effects of the produced NPs gave rise to the hypothesis that biosynthesized Ag-doped CuO NPs could aid in the seek for alternative chemotherapy agents [39]. Lower quantities of Ag-doped CuO NPs produced by green synthesis may have harmful effects because of the plant materials linked to the AgNPs and CuNPs [40]. Our findings showed that both the Ag-doped CuO NPs and *E. intermedia* extract had a remarkable anticancer activity in a dose-dependent manner, in which the anti-cancer effects of the doped NPs were greatly higher than that of extract alone. The findings of this study are very strongly corroborated by several data points, demonstrating the cytotoxic activity of biosynthesized AgNPs by *Juniperus*

chinensis extract against the lung cancer A549 cell line, *Sisymbrium irio* extracts against the HeLa cancer cell line [41], *Acacia nilotica* against colon cancer cells [42], biosynthesized CuNPs using *Yerba mate* extract against lung cancer A549 cell line [43], pumpkin seed extract against MDA-MB-231 breast cancer cell line [44], and Ag-doped CuO NPs against HaCaT human skin cancer cells *in-vitro* [45].

Our results indicated that extract alone had a lower impact on the alteration of anti-apoptotic and pro-apoptotic genes associated with cell death pathway, but the green-synthesized Ag-doped CuO NPs could alter the mRNA expression of all related-apoptosis genes, such as *caspase 3*, *Bax*, *P53*, and *Bcl2*, which leads to apoptosis in PC-3 cell lines. Similar results were obtained for green-synthesized AgNPs and CuNPs on the change of pro- and anti-apoptotic genes [46-50].

Mitochondrion-centered cell death named intrinsic apoptosis is due to the permeabilization of the mitochondrial outer membrane (MOMP), leading to the activation of caspase-9, the generation of apoptosomes, and the following stimulation of effector caspases. Extrinsic apoptosis can be started by transmembrane death receptors, but intracellular stress and growth factor removal cause apoptosis via the intrinsic apoptosis pathway. The BCL-2 and caspase categories of proteins control the initiation and termination of these processes [51].

Regulation of BCL-2 family members (*Bak* and *Bax*) causes MOMP and the discharge of pro-apoptotic proteins, like cytochrome C, into the cytosol from the intermembrane shortage [52]. When Apaf-1 is bound by cytochrome C, the apoptosomes are generated and caspase-9 is activated. Caspases 3 and 7 are promptly cleaved and activated by caspase-9 when it is active [53]. The characteristic features of the breakdown phase of cell death, such as DNA fragmentation, cell shrinkage, and membrane blebbing [54], are triggered by effector caspases. Additional mRNAs involved in the process of cell-killing were investigated after a study of the gene expression of initiator caspases. Within the examined mRNAs, *p53* is primarily involved in cell cycle arrest, aging, and apoptosis [55]. *Bax* can cause cancer cells to undergo apoptosis and is a pro-apoptotic mediator of *p53*. A prevalent way for apoptosis to take place is the overexpression of pro-apoptotic Bcl-2 family members by *p53*. Together with *p53*, pro-apoptotic

effector proteins with BH1, BH2, and BH3 domains and BH3-only proteins (famous for inhibiting anti-apoptotic Bcl-2) tend to play important roles in the activation of apoptosis. These proteins may potentially trigger pro-apoptotic Bcl-2 signals. Intracellular cytosolic proteins, which are typically contained in the intermembrane shortage, can be released when BH3-only proteins alter the permeability of outer membrane of mitochondria [56, 57].

Cancer therapeutic methods frequently target the process of apoptosis. In this investigation, we have discovered that compared to the control and the *E. intermedia* extract alone, the Ag-doped CuO NPs could significantly boost apoptosis in PC-3 cells. The most well-known method for eliminating cancer cells is induction of apoptosis through anticancer treatment. By targeting pro- and anti-apoptotic proteins, the Ag-doped CuO NPs were considerably efficient in triggering apoptosis, showing potential as anticancer treatments. Furthermore, the synergistic action of Ag and Cu NPs as well as the nanoscale size of these particles are likely to cause a greater mortality of cells treated with Ag-doped CuO NPs [58-60]. The flow cytometry analysis has been previously indicated that green synthesized AgNPs using *Allium cepa* L [61] extract, *Ginkgo Biloba* extract [62], *Azadirachta indica* [63], and green synthesized CuNPs using *Annona muricata* extract [49], *Vitex altissima* [64] extract, and Ag–Cu alloy NPs [65] induced apoptosis via mitochondrial pathways in the different cancer types (Colon, cervical, lung, breast).

Oxidative stress is the primary factor driving apoptosis in cancer cells. It occurs due to free radicals generated in response to environmental stimuli. Metallic nanoparticles (NPs) induce oxidative stress, disrupt tumor suppressor genes, reduce mitochondrial potential, and initiate lipid peroxidation, ultimately leading to cell death [66]. We have declared that the green-produced Ag-doped CuO NPs over-produced the ROS in PC-3 cell lines more than the control and *E. intermedia* extract, which exhibit the antioxidant mechanism in the induction of apoptosis in cancerous cells. AgNPs can produce ROS in the NIH3T3 cell and promote intrinsic apoptosis by stimulating the JNP route [67]. Free radicals (ROS) are generated by biological processes as a result of regular cell activity. The dysfunction of the biological processes that lead to DNA damage, cell cycle

arrest, lipid peroxidation, caspase activation, and apoptosis is triggered by the aberrant quantity of ROS [68]. ROS are produced by Fagonia indica-mediated AgNPs, according to research by Ullah et al., which modulates oxidative stress in MCF-7 cells [46]. Another findings revealed that HeLa cancer cells treated with Nepeta deflersiana-mediated AgNPs had significantly higher levels of ROS and lipid peroxidation, as well as lower levels of MMP and glutathione [69]. It has been demonstrated that the CuONPs cause cytotoxicity and genotoxicity in living things by releasing ROS [70, 71]. Several studies suggested that CuONPs might stimulate ROS generation in many cancer cells, including HepG293 and MCF-7 cells [72, 73]. A further investigation found that HepG2 cancer cells receiving biosynthesized CuONPs at 25–100 µg/mL for 48 hr produced more ROS than control cells [74]. According to the latest research, Ag-doped CuO NPs treatment of human lung cancer A549 cell lines inhibited cell growth and enhanced cytological and morphological changes by an elevated amount of ROS formation in the NSCLC cell line [8].

Jacob et al. (2022) have successfully biosynthesized Bimetallic Cu-Ag nanocomposites using green methods with the aqueous extract of Carica papaya leaves. This was confirmed through various analytical techniques such as FT-IR, SEM, EDAX, and TEM, which provided insights into the optical properties and surface morphology of the NPs. The bimetallic Cu-Ag nanocomposites exhibited antibacterial and anti-cancerous activities. The details of these activities were reported in the study, showcasing the potential of these nanocomposites for biomedical applications [34]. Also, Manikandan et al (2023) have successfully biosynthesized hybrid silver-copper oxide nanocomposites (Ag-CuO NCs) utilizing Ocimum americanum L. by one pot green chemistry method. Ag-CuO NCs exhibited potent anti-proliferative activity against the A549 lung cancer cell line, with a low IC_{50} value of 2.8 ± 0.05 µg/mL. Staining and comet assays confirmed that the NCs hindered cancer cell progression, induced apoptosis, and caused cell cycle arrest at the G0/G1 phase [23]. The *Moringa oleifera* leaf extract has been previously used for the green synthesis of pure and Ag-doped CuO NPs at the different concentrations (5%, 10%, 15%, and 20%). XRD analysis revealed that the NPs were in the monoclinic phase with a mean crystallite

size ranging from 15.22 nm to 3.67 nm. SEM images showed that the NPs prevented particle size enlargement, and EDAX analysis confirmed the presence of Cu, O, and Ag elements. FT-IR spectroscopy identified biomolecules in the leaf extract responsible for the bio-reduction of the NPs. UV-vis absorption spectra showed peaks between 210 nm to 240 nm, indicating the energy bandgap increased with higher Ag doping concentrations. MTT assay demonstrated a potent cytotoxic activity of the synthesized NPs against human lung cancer A549 cells. The 20% Ag-doped CuO NPs exhibited the highest cytotoxicity with an IC50 value of 15 µg/mL. Cell death has been induced through apoptosis, inhibiting cell proliferation, and causing morphological and cytological alterations, along with increased ROS accumulation in the A549 cell line [19]. Also, in a study by Doman, Ag-NPs and CuO-NPs have been successfully synthesized using *Spirulina platensis* as a reducing and capping agent. Ag-NPs had a spherical shape with sizes ranging from 2.23 nm to 14.68 nm, while CuO-NPs were smaller with sizes between 3.75 nm and 12.4 nm. UV/Vis spectroscopy confirmed the formation of Ag-NPs and CuO-NPs with λmax values of 425 nm and 234 nm, respectively. XRD and TEM further characterized the NPs. Ag-NPs and CuO-NPs were tested for their anticancer properties on various cancer cell lines (A549, HCT, Hep2) and normal cells (WISH). The IC_{50} values for Ag-NPs ranged from 3.8 µg/mL to 15.67 µg/mL, while for CuO-NPs, they ranged from 3.98 µg/mL to 54.59 µg/mL against the different cell lines [32].

It has been demonstrated that a family of NOS enzymes found in mammalian cells may produce NO, and each member of the family needs a variety of precursors and co-factors to operate properly [75]. Through the production of peroxynitrite (ONOO-) and N_2O_3, NO can harm DNA. Peroxynitrite can oxidize and nitrate DNA. It can also possibly induce single-strand DNA breakage by attacking the sugar-phosphate backbone, which leads to cell death [76]. We have showed the highest NO production in PC-3 cell lines treated with the Ag-doped CuO NPs, which is a probable mechanism that trigger with apoptotic activity of prepared Ag-doped CuO NP. Stevens et al. have revealed for the first time that NO-releasing NPs reached the cytoplasm of the target cell and specialized to late lysosomes and endosomes, which can be used as anti-tumor

agents [76]. There are conflicting studies on role of NO in cancer cells. However, several studies have shown that NO prevents cancer progression by reducing tumor growth, angiogenesis, migration, metastasis, etc. [77].

CONCLUSION

We have discovered that oxidative stress induced by the Ag-doped CuO NPs leads to toxicity in PC-3 cell lines by. As the levels of Ag and Cu increased, the hazardous severity of Ag-doped CuO NPs also enhanced. The promotion of the apoptosis pathway (upregulation of proapoptotic genes and downregulation of anti-apoptotic genes), ROS overproduction, and stimulation of NO level may be the causes of the detrimental behavior of green-synthesized Ag-doped CuO NPs utilizing the *E. intermedia* extract in PC-3 cells. Overall, our research indicated that the Ag-doped CuO NPs are more effective than the extract alone as an anticancer treatment because they specifically annihilate cancer cells. The preliminary research on the particular toxic effects of green-synthesized Ag-doped CuO nano-complex toward cancer cells called for a more in-depth investigation of many cancer types as well as normal cells and in-vivo conditions. The excellent *in vitro* results encourage us to continue future *invivo* studies of Ag-doped CuO NPs.

Credit authorship contribution statement

Azadeh Mohammadgholi contributed to the study's conception and design, supervised the study, and managed the project's execution. Parisa Raisi Dehkordi performed material preparation, data collection, and analysis. Nastaran Asghari Moghaddam contributed to the study's conception and design and participated in manuscript drafting. The first draft of the manuscript was written by Parisa Raisi Dehkordi, and all authors, approved the final manuscript.

CONFLICTS OF INTEREST

The authors declare that there are no conflicts of interest in this work.

ACKNOWLEDGMENTS

REFERENCES

1 Abdellatif AA, Abdelfattah A, Bouazzaoui A, Osman SK, Al-Moraya IS, Showail AMS, et al. Silver nanoparticles stabilized by poly (vinyl pyrrolidone) with potential anticancer activity towards prostate cancer. Bioinorg Chem Appl. 2022;2022:6181448.

2. Siege R, Miller K, Jemal A. Cancer statistics, 2016. CA Cancer J Clin. 2016;66(1):7-30.

3. Siegel Rebecca L, Miller Kimberly D. Jemal Ahmedin. Cancer statistics, 2019. CA: Cancer J Clin. 2019;69(1):7-34.

Wang B, Hu S, Teng Y, Chen J, Wang H, Xu Y, et al. Current advance of nanotechnology in diagnosis and treatment for malignant tumors. Sig Transduct Target Ther 2024;9: 200

5. Sun W, Deng Y, Zhao M, Jiang Y, Gou J, Wang Y, et al. Targeting therapy for prostate cancer by pharmaceutical and clinical pharmaceutical strategies. J Control Release. 2021;333:41-64.

6. Hojabri M, Tayebi T, Kasravi M, Aghdaee A, Ahmadi A, Mazloomnejad R, et al. Wet-spinnability and crosslinked Fiber properties of alginate/hydroxyethyl cellulose with varied proportion for potential use in tendon tissue engineering. In J Biol Macromol 2023;240:124492.

7. Noorbazargan H, Amintehrani S, Dolatabadi A, Mashayekhi A, Khayam N, Moulavi P, et al. Anti-cancer & anti-metastasis properties of bioorganic-capped silver nanoparticles fabricated from Juniperus chinensis extract against lung cancer cells. AMB Express. 2021;11(1):61.

8. Preethi DRA, Prabhu S, Ravikumar V, Philominal A. Anticancer activity of pure and silver doped copper oxide nanoparticles against A549 Cell line. Mater Today Commun. 2022;33:104462.

9. Katarzyńska-Banasik D, Kozubek A, Grzesiak M, Sechman A. Effects of silver nanoparticles on proliferation and apoptosis in granulosa cells of chicken preovulatory follicles: An *In vitro* study. Animals. 2021;11(6):1652.

10. Shaaban MT, Mohamed BS, Zayed M, El-Sabbagh SMJBb. Antibacterial, antibiofilm, and anticancer activity of silver-nanoparticles synthesized from the cell-filtrate of Streptomyces enissocaesilis. BMC Biotechnol 2024;24(1):1-13.

11. Andleeb A, Andleeb A, Asghar S, Zaman G, Tariq M, Mehmood A, et al. A systematic review of biosynthesized metallic nanoparticles as a promising anti-cancer-strategy. Cancers (Basel). 2021;13(11):2818.

12. Sangour MH, Ali IM, Atwan ZW, Al Ali AAAL. Effect of Ag nanoparticles on viability of MCF-7 and Vero cell lines and gene expression of apoptotic genes. Egypt J Med Hum Genet 2021;22 (9):1-11.

13. Bin-Jumah M, Al-Abdan M, Albasher G, Alarifi S. Effects of green silver nanoparticles on apoptosis and oxidative stress in normal and cancerous human hepatic cells *in vitro*. Int J Nanomed. 2020;15:1537-1548.

14. Moulavi P, Noorbazargan H, Dolatabadi A, Foroohimanjili F, Tavakoli Z, Mirzazadeh S, et al. Antibiofilm effect of green engineered silver nanoparticles fabricated from Artemisia scoporia extract on the expression of icaA and icaR genes against multidrug-resistant Staphylococcus aureus. J Basic Microbiol. 2019;59(7):701-712.

15. Danciu C, Muntean D, Alexa E, Farcas C, Oprean C, Zupko I, et al. Phytochemical characterization and evaluation of the antimicrobial, antiproliferative and pro-apoptotic potential of Ephedra alata Decne. hydroalcoholic extract against the MCF-7 breast cancer cell line. Molecules. 2018;24(1):13.

16. Sioud F, Dhouafi Z, Lahmar A, Elgueder D, Chekir-Ghedira L. A novel anticancer effect of Ephedra alata Decne in breast cancer cells. Nutr Cancer. 2022;74(9):3403-3412.

17. Nasar MQ, Shah M, Khalil AT, Kakar MQ, Ayaz M, Dablool AS, et al. Ephedra intermedia mediated synthesis of biogenic silver nanoparticles and their antimicrobial, cytotoxic and hemocompatability evaluations. Inorg Chem Commun 2022;137:109252.

18. Nasar MQ, Zohra T, Khalil AT, Ovais M, Ullah I, Ayaz M, et al. Extraction optimization, Total Phenolic-Flavonoids content, HPLC-DAD finger printing, antimicrobial, antioxidant and cytotoxic potentials of Chinese folklore Ephedra intermedia Schrenk & CA Mey. Braz J Pharma Sci 2023;58.

19. Preethi DRA, Prabhu S, Ravikumar V, Philominal AJMTC. Anticancer activity of pure and silver doped copper oxide nanoparticles against A549 Cell line. Mater Today Commun 2022;33:104462.

20. Chen W, Yang W, Chen P, Huang Y, Li FJAam, interfaces. Disulfiram copper nanoparticles prepared with a stabilized metal ion ligand complex method for treating drug-resistant prostate cancers. ACS Appl Mater Interfaces 2018;10(48):41118-41128.

21. Prashanth G, Sathyananda H, Prashanth P, Gadewar M, Mutthuraju M, Prabhu SB, et al. Controlled synthesis of Ag/CuO nanocomposites: evaluation of their antimycobacterial, antioxidant, and anticancer activities. Appl Phys A 2022;128(7):614.

22. Alnuwaiser MA, Betageri VS, Khan MI, Guedri KJJotICS. Facile synthesis of silver doped-copper oxide nano materials utilizing areca catechu (AC) leaf extract and their antidiabetic and anticancer studies. J Indian Chem Soc 2022;99(9):100606.

23. Manikandan DB, Arumugam M, Sridhar A, Perumalsamy B, Ramasamy TJER. Sustainable fabrication of hybrid silver-copper nanocomposites (Ag-CuO NCs) using Ocimum americanum L. as an effective regime against antibacterial, anticancer, photocatalytic dye degradation and microalgae toxicity. Environ Res. 2023;228:115867.

24. Afrand M, Sourinejad I, Fazeli SAS, Akbarzadeh A. Identification of Engraulids (Encrasicholina punctifer and E. pseudoheteroloba) using the COI gene as a DNA barcoding marker. J Aquatic Ecol 2018;7(3):39-47.

25. Chen J, Li S, Luo J, Wang R, Ding W. Enhancement of the antibacterial activity of silver nanoparticles against phytopathogenic bacterium Ralstonia solanacearum by stabilization. J Nanomater. 2016;2016.

26. Ng NS, Ooi L. A simple microplate assay for reactive oxygen species generation and rapid cellular protein normalization. Bio Protoc 2021;11(1):e3877

27. Naderi N, Mohammadgholi A, Asghari Moghadaam N. Anticancer Effects in HepG2 Cell Line: Apoptosis-Related Genes Analysis and Nitric Oxide Level Investigations. IJMCM. 2024; 13(3):303-324.

28. Ahmadi S, Seraj M, Chiani M, Hosseini S, Bazzazan S, Akbarzadeh I, et al. *In vitro* development of controlled-release nanoniosomes for improved delivery and anticancer activity of letrozole for breast cancer treatment. 2022;17:6233.

29. Akhilesh R, Amith S, Absar A, Murali S. Role of halide ions and temperature on the morphology of biologically

synthesized gold nanoparticles. Langmuir. 2006;22:736-741.

30. Borchert H, Shevchenko EV, Robert A, Mekis I, Kornowski A, Grübel G, et al. Determination of nanocrystal sizes: a comparison of TEM, SAXS, and XRD studies of highly monodisperse CoPt3 particles. Langmuir. 2005;21(5):1931-1936.

31. Vidhya S, Rose AL. Microwave Assisted Green Synthesis of Gold Nanoparticles Using Bougainvillea glabra Leaf Extract. Asian J Chem. 2017;29(8).

32. Amatori S, Persico G, Fanelli M. Real-time quantitative PCR array to study drug-induced changes of gene expression in tumor cell lines. J Cancer Metastasis Treat. 2017;3(90):10.20517.

33. Nel A, Xia T, Madler L, Lin N. Ti is an abundant element in soil and appears in a variety of forms including primary and secondary minerals as well as organically bound and amorphous compounds. Sci. 2006;311:622-627.

34. Rasool S, Tayyeb A, Raza MA, Ashfaq H, Perveen S, Kanwal Z, et al. Citrullus colocynthis-mediated green synthesis of silver nanoparticles and their antiproliferative action against breast cancer cells and bactericidal roles against human pathogens. Nanomater. 2022;12(21):3781.

35. Abd El-Aziz SM, Farahat EAJJoI, Polymers O, Materials. The Activity of Vossia cuspidata Polysaccharides-Derived Monometallic CuO, Ag, Au, and Trimetallic CuO-Ag-Au Nanoparticles Against Cancer, Inflammation Wound Healing. 2023;33(3):853-865.

36. Giridasappa A, Ismail SM, Gopinath S. Antioxidant, Bactericidal, Antihemolytic, and Anticancer Assessment Activities of Al2O3, SnO2, and Green Synthesized Ag and CuO NPs. Handbook of Sustainable Materials: Modelling, Characterization, and Optimization: CRC Press; 2023367-202398.

37. Doman KM, Gharieb MM, Abd El-Monem AM, Morsi HHJIJoEHR. Synthesis of silver and copper nanoparticle using Spirulina platensis and evaluation of their anticancer activity. Int J Environ Health Res. 2024;34(2):661-673.

38. Aarya, Thomas T, Sarangi BR, Sen Mojumdar SJAo. Rapid Detection of Ag (I) via Size-Induced Photoluminescence Quenching of Biocompatible Green-Emitting, l-Tryptophan-Scaffolded Copper Nanoclusters. ACS Omega. 2023;8(16):14630-14640.

39. Jacob J, Prasad T, Vithiya B, Athisa MRJJoP, Microbiology A. Biosynthesis of Bimetallic Cu-Ag Nanocomposites and Evaluation of their Electrocatalytic, Antibacterial and Anti-Cancerous Activity. J Pure Appl Microbiol.2022;16(2):955-966.

40. Botcha S, Prattipati SD. Callus extract mediated green synthesis of silver nanoparticles, their characterization and cytotoxicity evaluation against MDA-MB-231 and PC-3 cells. BioNanoSci. 2020;10:11-22.

41. Mosdam T. Rapid colorimetric assay for cellular growth and survival: application to proliferation and cytotoxic assay. J Immunol Methods. 1983;65:55-63.

42. Farah MA, Ali MA, Chen S-M, Li Y, Al-Hemaid FM, Abou-Tarboush FM, et al. Silver nanoparticles synthesized from Adenium obesum leaf extract induced DNA damage, apoptosis and autophagy via generation of reactive oxygen species. Colloids and Surfaces B: Biointerfaces. 2016;141:158-169.

43. Rizwana H, Bokahri NA, Alfarhan A, Aldehaish HA, Alsaggabi NS. Biosynthesis and characterization of silver nanoparticles prepared using seeds of Sisymbrium irio and evaluation of their antifungal and cytotoxic activities. Green Process Synthesis. 2022;11(1):478-491.

44. Alduraihem NS, Bhat RS, Al-Zahrani SA, Elnagar DM, Alobaid HM, Daghestani MH. Anticancer and antimicrobial activity of silver nanoparticles synthesized from pods of Acacia nilotica. Processes. 2023;11(2):301.

45. Majid A, Faraj HR. Green Synthesis of Copper Nanoparticles using Aqueous Extract of Yerba Mate (Ilex Paraguarients St. Hill) and its Anticancer Activity. Int J NanosciNanotechnol. 2022;18(2):99-108.

46. Zughaibi TA, Mirza AA, Suhail M, Jabir NR, Zaidi SK, Wasi S, et al. Evaluation of anticancer potential of biogenic copper oxide nanoparticles (CuO NPs) against breast cancer. J Nanomater. 2022;2022:1-7.

47. Rajendran R, Mani A. Photocatalytic, antibacterial and anticancer activity of silver-doped zinc oxide nanoparticles. J Saudi Chem Soc. 2020;24(12):1010-1024.

48. Ullah I, Khalil AT, Ali M, Iqbal J, Ali W, Alarifi S, et al. Green-synthesized silver nanoparticles induced apoptotic cell death in MCF-7 breast cancer cells by generating reactive oxygen species and activating caspase 3 and 9 enzyme activities. Oxid Med Cell Longev. 2020;2020:1215395.

49. Plackal Adimuriyil George B, Kumar N, Abrahamse H, Ray SS. Apoptotic efficacy of multifaceted biosynthesized silver nanoparticles on human adenocarcinoma cells. Scientific reports. 2018;8(1):14368.

50. Biresaw SS, Taneja P. Copper nanoparticles green synthesis and characterization as anticancer potential in breast cancer cells (MCF7) derived from Prunus nepalensis phytochemicals. Mater Today: Proceedings. 2022;49:3501-3509.

51. Mahmood RI, Kadhim AA, Ibraheem S, Albukhaty S, Mohammed-Salih HS, Abbas RH, et al. Biosynthesis of copper oxide nanoparticles mediated Annona muricata as cytotoxic and apoptosis inducer factor in breast cancer cell lines. Sci Rep. 2022;12(1):16165.

52. Aishajiang R, Liu Z, Wang T, Zhou L, Yu D. Recent Advances in Cancer Therapeutic Copper-Based Nanomaterials for Antitumor Therapy. Molecules. 2023;28(5):2303.

53. Galluzzi L, Vitale I, Abrams J, Alnemri E, Baehrecke E, Blagosklonny M, et al. Molecular definitions of cell death subroutines: recommendations of the Nomenclature Committee on Cell Death 2012. Cell Death Different. 2012;19(1):107-120.

54. Zuckerkandl E, Pauling L. Evolutionary divergence and convergence in proteins. Evolving genes and proteins: Elsevier; 1965. p. 97-166.

55. Srinivasula SM, Ahmad M, Fernandes-Alnemri T, Alnemri ES. Autoactivation of procaspase-9 by Apaf-1-mediated oligomerization. Molecular cell. 1998;1(7):949-957.

56. Brentnall M, Rodriguez-Menocal L, De Guevara RL, Cepero E, Boise LH. Caspase-9, caspase-3 and caspase-7 have distinct roles during intrinsic apoptosis. BMC Cell Biol. 2013;14:1-9.

57. Amaral JD, Xavier JM, Steer CJ, Rodrigues CM. The role of p53 in apoptosis. Discov Med. 2010;9(45):145-152.

58. Bao J, Jiang Z, Ding W, Cao Y, Yang L, Liu J. Silver nanoparticles induce mitochondria-dependent apoptosis and late non-canonical autophagy in HT-29 colon cancer cells. Nanotechnol Rev. 2022;11(1):1911-1926.

59. Kasravi M, Yaghoobi A, Tayebi T, Hojabri M, Taheri AT, Shirzad F, et al. MMP inhibition as a novel strategy for extracellular matrix preservation during whole liver decellularization. Biomater Adv. 2024:213710.

60. Ghosal K, Ghosh S, Ghosh D, Sarkar K. Natural polysaccharide derived carbon dot based in situ facile green synthesis of silver nanoparticles: Synergistic effect on breast cancer. Int J Biol Macromol. 2020;162:1605-

1615.

61. Bélteky P, Rónavári A, Zakupszky D, Boka E, Igaz N, Szerencsés B, et al. Are smaller nanoparticles always better? Understanding the biological effect of size-dependent silver nanoparticle aggregation under biorelevant conditions. Int J Nanomed. 2021; 22:3021-3040.

62. Nishanthi R, Malathi S, Palani P. Green synthesis and characterization of bioinspired silver, gold and platinum nanoparticles and evaluation of their synergistic antibacterial activity after combining with different classes of antibiotics. Mater Sci Eng: C. 2019;96:693-707.

63. Abdellatif AA, Mahmood A, Alsharidah M, Mohammed HA, Alenize SK, Bouazzaoui A, et al. Bioactivities of the green synthesized silver nanoparticles reduced using Allium cepa L aqueous extracts induced apoptosis in colorectal cancer cell lines. J Nanomater. 2022;2022:1-13.

64. Xu Z, Feng Q, Wang M, Zhao H, Lin Y, Zhou S. Green biosynthesized silver nanoparticles with aqueous extracts of ginkgo biloba induce apoptosis via mitochondrial pathway in cervical cancer cells. Front Oncol. 2020;10:575415.

65. Alharbi NS, Alsubhi NS. Green synthesis and anticancer activity of silver nanoparticles prepared using fruit extract of Azadirachta indica. J Radiation Res Appl Sci. 2022;15(3):335-345.

66. Bhavana S, Kusuma C, Gubbiveeranna V, Sumachirayu C, Ravikumar H, Nagaraju S. Green route synthesis of copper oxide nanoparticles using Vitex altissima [L] leaves extract and their potential anticancer activity against A549 cell lines and its apoptosis induction. Inorg Nano-Metal Chem. 2022:1-14.

67. Al Tamimi S, Ashraf S, Abdulrehman T, Parray A, Mansour SA, Haik Y, et al. Synthesis and analysis of silver–copper alloy nanoparticles of different ratios manifest anticancer activity in breast cancer cells. Cancer Nanotechnol. 2020;11:1-16.

68. Hsin Y-H, Chen C-F, Huang S, Shih T-S, Lai P-S, Chueh PJ. The apoptotic effect of nanosilver is mediated by a ROS-and JNK-dependent mechanism involving the mitochondrial pathway in NIH3T3 cells. Toxicol Letters. 2008;179(3):130-139.

69. Thannickal VJ, Fanburg BL. Reactive oxygen species in cell signaling. American Journal of Physiology-Lung Cellular Mol Physiol. 2000;279(6):L1005-L1028.

70. Al-Sheddi ES, Farshori NN, Al-Oqail MM, Al-Massarani SM, Saquib Q, Wahab R, et al. Anticancer potential of green synthesized silver nanoparticles using extract of Nepeta deflersiana against human cervical cancer cells (HeLA). Bioinorganic Chem Appl. 2018;2018.

71. Shafagh M, Rahmani F, Delirezh N. CuO nanoparticles induce cytotoxicity and apoptosis in human K562 cancer cell line via mitochondrial pathway, through reactive oxygen species and P53. Iranian J Basic Med Sci. 2015;18(10):993.

72. Tabrez S, Khan AU, Mirza AA, Suhail M, Jabir NR, Zughaibi TA, et al. Biosynthesis of copper oxide nanoparticles and its therapeutic efficacy against colon cancer. Nanotechnol Rev. 2022;11(1):1322-1331.

73. Fu X. Oxidative stress induced by CuO nanoparticles (CuO NPs) to human hepatocarcinoma (HepG2) cells. J Cancer Ther. 2015;6(10):889.

74. Ali K, Saquib Q, Ahmed B, Siddiqui MA, Ahmad J, Al-Shaeri M, et al. Bio-functionalized CuO nanoparticles induced apoptotic activities in human breast carcinoma cells and toxicity against Aspergillus flavus: an *in vitro* approach. Process Biochem. 2020;91:387-397.

75. Liu Y, Zeng Z, Jiang O, Li Y, Xu Q, Jiang L, et al. Green synthesis of CuO NPs, characterization and their toxicity potential against HepG2 cells. Mater Res Express. 2021;8(1):015011.

76. Xu W, Liu LZ, Loizidou M, Ahmed M, Charles IG. The role of nitric oxide in cancer. Cell Res. 2002;12(5):311-320.

77. Stevens EV, Carpenter AW, Shin JH, Liu J, Der CJ, Schoenfisch MH. Nitric oxide-releasing silica nanoparticle inhibition of ovarian cancer cell growth. Mol Pharma. 2010;7(3):775-785.

78. Hickok JR, Thomas DD. Nitric oxide and cancer therapy: the emperor has NO clothes. Curr Pharma Design. 2010;16(4):381-391.